

Optimal Energy Management and Sizing of a Community Smart Microgrid Using GA with Demand Side Management and Load Uncertainty

Maneesh Kumar¹ and Barjeev Tyagi²

ABSTRACT: This paper presents an optimal energy management and sizing study for a smart community microgrid (MG) with the uncertainty considerations in load demand. For this purpose, an isolated small scale microgrid is considered. It has no access to the main supply grid and serves a small community of 15 houses located in a remote area. The loads are divided into controllable and uncontrollable categories. Demand side management (DSM) is utilized to produce a feasible alteration in the controllable part of the load. These alterations can be implemented with the help of smart devices connected in the consumers' premises. The overall problem is formulated to fix the optimal size of the distributed energy resources (DERs) required in the MG by using a genetic algorithm (GA) to minimize the net cost-based optimization problem. A diesel generator based power plant and a battery storage power plant have been considered as the DER unit. The overall optimization is performed in two parts. The first part of optimization is done without DSM implementation, and the second part is done on the modified system peak load after DSM implementation. A numerical case study has been performed to obtain the quantitative results and to check the effectiveness of the formulated algorithms in terms of the optimal number of DERs, their corresponding optimal ratings, optimal cost value, reduction in carbon footprint, and the annual cost savings in the form of CO_2 emission tax. A comparative study of the GA and the mixed-integer linear programming (MILP) approaches has also been conducted for finding the optimal cost. The overall study has been carried out under the MATLAB environment.

Keywords: Microgrids (MGs), Demand side management (DSM), Optimization, Carbon footprints, Renewable energy, Genetic algorithm (GA)

DOI: 10.37936/ecti-cit.2021152.240491

Article history: received April 22, 2020; revised July 17, 2020; accepted September 15, 2020; available online April 23, 2021

1. INTRODUCTION

Microgrids (MGs), from the viewpoint of overall system reliability improvement as well as for the utilization of renewable energy resources (RESs), are potentially viable. These grids not only support the main grid, but also provide a reliable supply to remotely located communities where the main grid supply may not be available. Microgrids are of two types, grid-connected/supported and Isolated/islanded microgrids. In grid supported MGs, voltage and frequency are controlled by the main supply grid, whereas the islanded type of microgrids must be self-sufficient to produce enough power to feed load re-

quirements. For an economically viable MG, it is important to formulate an optimal energy management and sizing problem. That includes fixed and variable costs involved in MG planning. Therefore, planning and operation of an MG depends upon many factors which involve estimation of load, available distributed generation estimation, and also site availability [1].

In this paper, capital costs (\$/kW), operation & maintenance costs (\$/kW), and the fuel costs associated with the diesel power plant (DPP) are considered. The formulated objective function in the study is a cost minimization function and the overall optimization is performed with the help of a GA. The

^{1,2}The authors are with Department of Electrical Engineering, IIT Roorkee, Roorkee, India., E-mail: mkumar2@ee.iitr.ac.in and barjeev.tyagi@ee.iitr.ac.in

annual cost savings is obtained through a comparison between pre and post implementation of DSM. A DSM is referred to as the alteration in load when and if required for maximum utilization of resources as well as to improve the load profile of the consumer. In this paper, historical data of the load has been considered for forecasting purposes. A multi-layer feed-forward (FF) neural network trained with back-propagation (BP) algorithm [2], [3] is used.

1.1 Literature Review

For long term MG planning, economically viable configurations of DRs along with cost benefits are needed. RESs are becoming important choices to get cheaper and cleaner energy. The increasing renewable penetration in the microgrid system decreases the carbon footprints, but it also decreases the overall system reliability. On the other hand, the use of RESs such as wind energy, solar energy, biomass energy, etc., reduces the overall running as well as operation costs [4,5] of a microgrid system. It is quite important to identify the costs associated with the MG system. The cost data associated with energy generation in MG is specified in [6]. As given in [7] and [8], the non-OECD (Organization for Economic Cooperation and Development) countries that shows the developing countries need most of the power consumption by 2040. Hence, the utilization of RESs is growing remarkably to match the increasing load demands. An example of this is India, where a target of 100 GW of energy generation from RESs by 2022 has been set by the government. It also affects the gross domestic production (GDP) of any country [9]. In [10], cost-based MG planning is proposed that encompasses a communication-based study of short and long term MG planning. [11] proposed a study which is based upon the associated risk factors in the MG planning to get enhanced policy incentives. [12] proposed an interconnected MG planning framework to reduce overall MG system costs. In [13], an energy management scenario is presented for Li-ion based storage systems utilizing a cost reduction problem for MG. [14] proposed an optimal diesel generation problem utilizing virtual storage available on the load side. The majority of the available studies considered a single scenario based deterministic approach and neglect any kind of uncertainty associated with the MG systems.

For an optimal and prevailing MG planning solution, appropriate load forecasting is also vital. [15,16] proposed a load forecasting method that depends upon a memory-based deep learning process. Compared to different traditional load forecasting methods, [17] proposed an IoT (Internet of Things) based load forecasting which offers more accurate data weight. An accurate load forecasting approach is proposed in [18] which uses a differential algorithm based rule sets for minimizing the forecasting errors. An optimal energy management technique is proposed

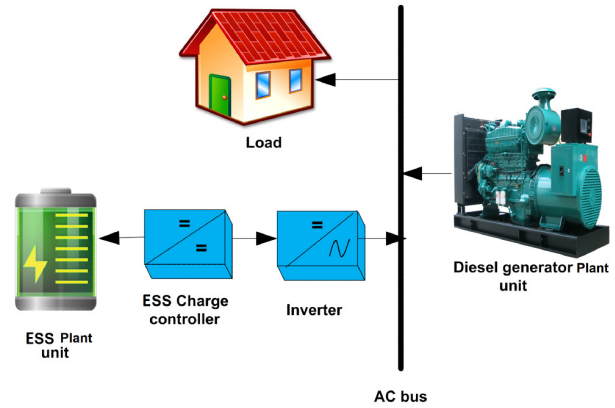


Fig.1: MG structure under consideration

in [19], where a one-layer recurrent neural network is used. The battery storage has been modeled to support the energy balance in the smart grid as an important part of the study. An improved technique for long-term load forecasting which is based upon wavelet and neural community is proposed in [20]. In [21], characteristics of the load time-series of a typical MG are discussed, and the differences with the load-time series of traditional power systems are described. [22] examines the most admissible and acceptable studies on electricity demand predictions over the last forty years and presents the different models used as well as future trends. [23] proposed short-term forecasting of electrical energy demands at the local level, incorporating advanced metering infrastructure (AMI), or smart-meter data.

The prescribed study associates the use for (DSM) to reduce the burden on connected energy sources as well as to improve the overall system load factor. It is important to consider and implement a typical DSM technique. In general, the demand side management or demand response (DR) are the techniques and methodologies that encourage the consumer to reduce their energy consumption optimally [24]. DSM has many advantages. However, it is still underutilized. [25] provides a framework for investment and operation of a microgrid underneath renewable penetration along with DSM. [26] proposes small microgrid planning with energy management and MG optimization. An optimal microgrid planning and operation problem has been formulated in [27-29] using DSM with renewable penetration. Here, a bi-objective problem is formulated for the economic as well as the environmental aspects. In [30], a simulated annealing based approach is utilized for MG planning. It is proposed in [31] that DSM is also a desirable feature when it considers an overall MG control design.

Although comprehensive literature in the field of optimal microgrid planning and energy management is available as given above, most of them consider a deterministic approach. Moreover, this study encourages the use of smart technologies for the energy

savings in the system. This study also emphasizes the formulation of an optimal problem that leads to a reduction in carbon emission. The execution of DSM in this paper is carried out through the use of recursive programming, and the peak shaving method is utilized for this purpose. The peak shaving method is defined as the peak load reduction on a utility during peak periods by shifting the peak load to the low load areas. It can be applied through direct control of consumer appliances or by way of electricity control through consumer's smart devices. A central controller is assigned this task, which is placed between the load and the distributed generation. Two kinds of objective functions exist: one is to enhance load factor for utility, and the other is to reduce electricity bills for consumer's [32]. Half an hour forecasted data samples are considered in this paper to obtain the MG load profile. The MG structure prescribed in this paper is given in figure 1, wherein two sources are considered. One is diesel engine generator based that also serves as a primary source. The other is a storage plant unit that supports the primary source to reduce the carbon footprints (CFP). The overall contribution of the study is given in the next subsection.

1.2 Contribution

Most of the available literature considers a deterministic planning approach for the optimal problem formulation, but somehow neglects the randomness in the load demand data. The use of smart technologies for MG planning needs more attention and research. The formulation of the overall optimization problem is carried out in two parts. These two parts are associated with the DSM implementation strategy which focuses on the controllable load of the MG system in a simpler manner through the smart devices.

The distinctiveness of the algorithm for the DSM implementation may be observed from its functioning with various load profiles since it considers the percentage contribution of individual household load in the formation of an overall system peak. It means each individual load curve has a certain percentage contribution in the formation of the overall system load curve. At each iteration of the algorithm, it finds which individual house load curve contributes the maximum percentage in the MG system peak and accordingly it shifts the peak load of that household load to the low load areas of the load profile curve. This paper proposes a more generalized and simple methodology to address the MG planning problem for remote communities. In this study, the utilization of demand response along with the minimization of CFP has also been encouraged. The overall objective of the study is to formulate the optimal energy solutions for remotely situated communities which require comparatively less time to establish and also have adopted an energy saving strategy in terms of

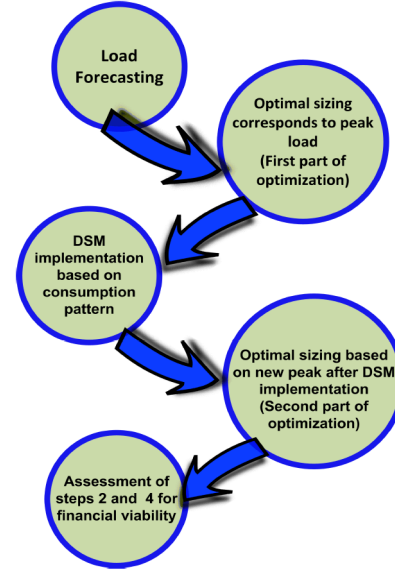


Fig.2: Steps involved in MG planning

demand side management. For the implementation, different algorithms are applied to get an optimal utilization of distributed energy resources. The results show the implementation of the formulated algorithms in coordination with the genetic algorithm which is used to optimize the cost minimization function.

The rest of the paper is arranged as follows. In section II, methodology and problem formulation is presented. In section III, a numerical case study has been conducted. In section IV, results are discussed, followed by the conclusion in section V.

2. METHODOLOGY AND PROBLEM DESCRIPTION

2.1 Methodology

The steps entailed in the overall planning and sizing are given in figure 2. The loads are divided into two categories: controllable (can be controlled through smart appliances or by any other mode), and uncontrollable loads (must be supplied continuously and are part of the base-load). The DSM is carried out over the controllable load part of the overall MG system load. The peak shaving approach is used for the DSM implementation as discussed in the last section. A storage system based plant has also been included in the MG test system.

The load forecasting is done through a multi layer feed-forward neural network trained with back propagation (BP) algorithm as shown in figure 3, where N_i , N_h , and N_o are the total number of variables pertaining to the input layer, hidden layer, and the output layer, respectively. The i^{th} input corresponding to the input layer and the j^{th} unit of the hidden layer are connected to each other through a factor W_{ij} which is known as a weighting factor. A nonlin-

ear transfer-

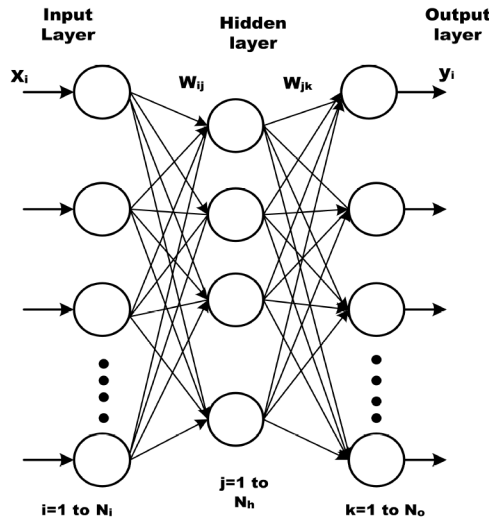


Fig.3: A Multilayer feed-forward neural network

formation is done by each unit of the hidden layer, known as neuron. The input corresponding to unit i is shown by x_i . The output of unit k of the neuron is shown by y_i . The weighting factor between neuron j and the neuron k is shown by W_{jk} . The Feed-forward neural network is trained to approximate a function between the half hourly load and the input variable. Next the procedure used to forecast the load is given. More details can be seen from [3-33]. The number of hidden layers and neurons can vary and depend upon the size and the nature of considered data set.

2.1.1 Selection of input variables

The Input variables viz. previous load, price, and temperatures are considered for testing and the training of ANN.

2.1.2 Pre-processing of the data

Here, the improper and error data is identified and discarded.

2.1.3 Scaling

The raw data is scaled between the lower and upper bands of the transfer function. Typically, between 0 & 1 or -1 & 1.

2.1.4 Training

An ANN system uses training to learn the patterns that are present in data.

2.1.5 Simulation

The input patterns are used to simulate the forecasting output data.

2.1.6 Post-processing of data

Only de-scaling of the data is required to obtain the forecasted load data.

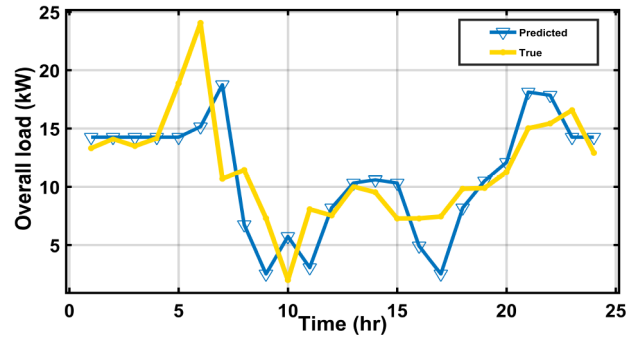


Fig.4: The overall load response curve of the micro-grid system

2.1.7 Analysis of the error

The overall output data is analyzed using different methods such as Mean Absolute Percentage Error (MAPE), Mean Square Error (MSE), and Percentage Error (PE) to obtain an error-free data. The performance parameters are obtained as: RMSE: 2.1; R-squared: 0.52; MSE: 3.1; MAPE: 1.23; training time: 0.985sec.

The load data has been forecasted with the help of the previously discussed method, and the load curve has been prepared. The historical data pertaining to load, temperature, and the energy price has been considered carefully during the forecasting process. The overall load curve of the microgrid system is obtained as a forecasted curve and is shown in figure 4. The predicted load curves are used as the microgrid individual house load curves. From these, the overall system load curve is obtained and can also be seen in figure 6(f) later in the section. The considered ANN approach has the following structure:

Network: Feed-forward back propagation

No. of inputs: 3

No. of hidden layers: 1

No. of hidden neurons: 10

Transfer function: Hidden layer - Tan-sigmoid; Output layer - Linear TF

Training function: Levenberg-Marquardt

Learning function: Gradient descent with momentum back propagation.

For simplicity, a few assumptions have also been made in this paper. For instance, the converter dynamics are disregarded from the storage system. The DPP and ESS plants are connected to an a.c bus and are feeding a small community load.

The step by step development of optimization involved in DSM implementation is given below. The overall optimization problem is designed as:

Step I. Load forecasting of 15 house community.

Step II. Get individual load curves and the overall load curve of the community.

Step III. Apply first part of optimization using GA here corresponding to the initial system peak load.

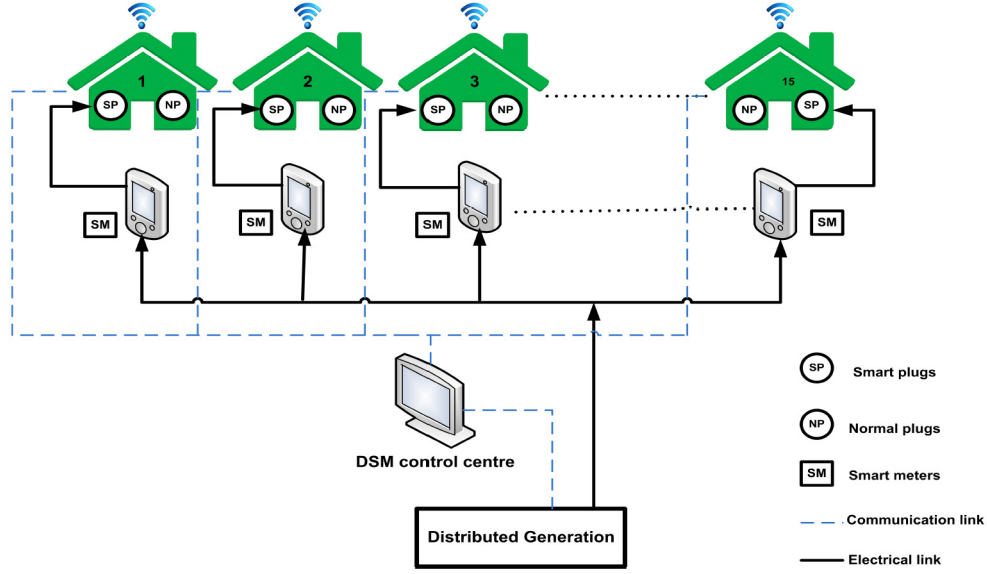


Fig. 5: Smart community scheme

Step IV. Obtain % contribution of each load curve in overall peak formation

Step V. Set a dispatchable limit of DERs for the DSM implementation.

Step VI. Apply DSM to set the load curve at the dispatchable limit.

Step VII. Apply second part of optimization using GA at this point.

The algorithm may be carried out for two seasonal scenarios, i.e., winter and summer seasons. In this paper, a winter scenario is considered with an assumption of peak load occurrence annually using the forecasting. The smart community scheme for DSM implementation is given in figure 5, where the controllable loads are connected to smart plugs (SP) and the remaining loads are connected with the normal plugs (NP). Wireless communication such as WiMax(IEEE 802.16, 802.22) standards; LTE/2G/3G cellular connectivity, home area network (HAN), WiFi (IEEE 802.11), ZigBee (IEEE 802.15.4), (IEEE 802.15.1), etc. or wired communication techniques can be used for load control or load alterations.

In this study, a wireless communication link is assumed to connect the smart community with a demand side control center. This controller is placed between the load and the distributed generation. The smart meters are connected between the controller and the loads to get load data for necessary control actions. The load curve of the individual houses and collective load profile curves of the whole system are given in figures 6a-6e and 6f, respectively, with randomness added. These are discussed later in this section.

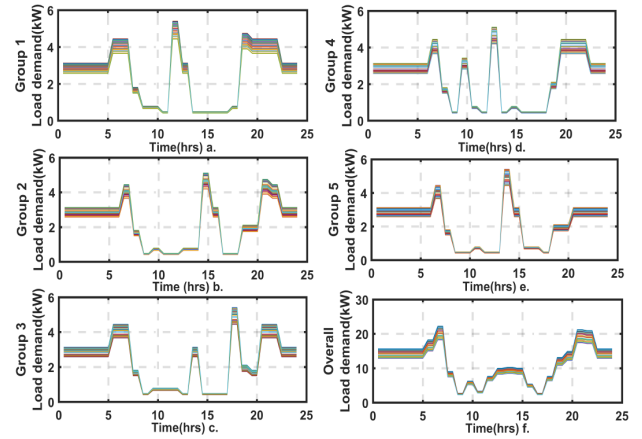


Fig. 6: Half hourly load curve of five individual group loads (a-e) and overall load curve (f).

2.2 Optimal Problem formulation

2.2.1 Optimal Microgrid Sizing

The overall objective function is formulated as a cost minimization function of the microgrid system that needs to be minimized with the help of a meta-heuristic approach to obtain an optimal size of a small community microgrid and is given in equation (1). This cost function includes installation costs, operation, and maintenance costs, and also the fuel costs associated with the DPP unit.

$$\min(f) = \min\left(\sum_{i=1}^N (CI_i + C_{om,i}) * Xr_i + C_{fuel} + C_{dsm}\right) \quad (1)$$

N represents the total number of distributed energy resources types connected to the microgrid system

with respect to a particular plant. ' CI_i ' (\$/kW) is the capital cost of the plant, ' C_{om} ' (\$/kW) represents the operation and maintenance cost of the plant. ' i ' is the i^{th} plant unit. ' X_r ' is the plant output rating. ' C_{fuel} ' is the fuel cost of DPP unit and is equals to $\sum_t^T \sigma_{dg} * X_{dg}(t)$. ' σ_{dg} ' (\$/kWh) is the fuel cost of a diesel generator unit and is considered as 0.25. ' $X_{dg}(t)$ ' is the diesel generator output in DPP at any time ' t '. ' T ' total sampling period and is considered as 24hrs. ' C_{dsm} ' is any cost associated with DSM implementation which includes cost of smart appliances or any other device. For simplicity of the algorithm, it is assumed that the DSM implementation cost can be recovered within a time period of 2-3 years. Therefore, this cost can be neglected from the objective function and hence, the objective function in equation (1) can be replaced by equation (2).

$$\min(f) = \min\left(\sum_{i=1}^N (CI_i + C_{om,i}) * X_{r_i} + C_{fuel}\right) \quad (2)$$

The genetic algorithm is being utilized to solve the optimization problem with a generation size of 200 and the constraint tolerance is set at 1.0e-03 with a crossover fraction of 0.8. The two types of DERs are considered for the study and typical cost considerations for these are given in Table 1 [34-37].

Table 1: Typical costs and ratings consideration for the DERs

S.No	DER	CI (\$/kW)	O _r (kW)	C _{fuel} (\$/kW)	C _{om} (\$/kW)
1.	DPP	692.3	10	0.23	0.8
2.	ESS	2272.7	10	0	0.27

2.2.2 Load modeling

The load is modeled as a random variable, and a beta distribution is being utilized to create the randomness in the load demand with the help of the 'randraw' function of MATLAB as shown in figure 6. The probability density function (PDF) is defined in equation (3).

$$PDF = \frac{(x-l)^{a-1} * (u-x)^{b-1}}{Z_{(a,b)} * (u-l)^{a+b-1}} \quad (3)$$

x is a variable. a and b are called shape parameters. l , and u are the lower and upper bounds of distribution respectively. $Z_{(a,b)}$ is a beta function which defined in equation (4).

$$Z_{(\alpha,\beta)} = \int_0^1 x^{(\alpha-1)} * (1-t)^{\beta-1} dt \quad (4)$$

α, β are the shape parameters and are considered as 0.5 [38]. The randomness or the uncertainty in the load has been added as a percentage of variation from the average load value. Therefore, a more practical

scenario can be presented with respect to the load demand. There have been 24 such scenarios added to each household load curve and these are shown in figure 6. For the ease of understanding how the algorithms work, it is assumed that out of total 15 community houses, every three houses have the same kind of load curve. This may be true because of the same kind of load connectivity in the houses or because of the same work profile of the community. Hence, there will be a total of five curves obtained and they are shown in the form of groups 1 to 5 in the figure.

2.2.3 Description of algorithms

The overall problem is formulated for a smart community with a small scale microgrid with the help of algorithms 1 and 2. Any available excess energy in the system corresponding to load variations or load reduction can be utilized to charge the storage system.

Algorithm 1 Demand Response Implementation

Input: Dispatchable limit (DL); Sampling period SP(=24 hrs)

Output: Modified Load Curve

Initialize iter=1;

while iter ≤ SP **do**

if $X_{peak} \geq DL$ **then**

Apply DSM using PSS;

Increment iter=iter+1;

return Obtain Modified Load Curve.

A dispatchable limit, which is variable with respect to the system load and the DERs ratings, is set for the DPP, shown in algorithm 1. This limit can be set as per generation availability after the fulfillment of the uncontrollable or critical part of the load as a percentage of the output power of the connected DERs and can be applied only on the controllable part of the load. This algorithm reduces the peak demand of the individual community loads to a predefined set dispatchable limit. For this purpose, the peak shaving strategy (PSS) is used.

Algorithm 2 ESS Support

Input: Modified Load Curve; I_{count} ; Initial SOC; SP(=24 hrs)

Output : SOC

Data: X_{dg}

Initialize count=1;

while count ≤ SP **do**

if $I_{count} \geq 0.85X_{dg}$ && SOC ≥ 0.3 **then**

Discharge Battery using Eq (5);

else if ($I_{count} < 0.85X_{dg}$) **then**

(**if** SOC < 0.9) **then**

Evaluate SOC_{count} ;

Set ISOC= SOC_{count} ;

Increment count=count+1;

else $SOC_{count} = ISOC$

else Charge Battery using Eq (5);

return Add output line

It is worth mentioning that the shifting of the peak load to the low load areas depends upon the percentage contribution of each load to create the overall peak of the system as discussed in section I. This process continues until all individual community peaks settle to a predefined dispatchable limit.

As soon as the load curve acquires the set dispatchable limit after the execution of DSM by using smart appliances connected in the system, the load is being supplied through the DPP being supported by the ESS plant. From the efficiency point of view, it is assumed that the DPP is running near 85-90% of its rated capacity.

The depth of discharge (DOD) for the storage system batteries is considered as 30%, and once the batteries have discharged to this value, they acquire a standby. If the charging area or excess energy (available in terms of % of load variations/reductions) are not available in the system, the ESS gets charge through a reserve capacity of the DPP i.e., X_{dgr} . This condition may occur with a large increment in the MG load. Each time when the charging regions are available, the ESS will charge through the DPP, and the process continues until the battery acquires a maximum charge level of 90%. After this, the battery system again acquires a condition of standby. The algorithms check the load demand at each instant for the whole 24 hrs of a typical day. The overall charging/discharging processes of the ESS system are accomplished through equations (5)-(8). It is assumed that the battery banks used in the ESS system have similar characteristics and ratings. I_{count} , as seen from the algorithm 2, is the instantaneous value of the load. SOC_{count} gives the storage system state of charge at any time instant. $ISOC$ is the initial state of charge which the ESS acquires after each iteration. Once the conditions considered in the given algorithm are fulfilled, the storage system supplies the power or starts discharging. It is assumed that the storage system is initially charged to its full capacity.

The net power flow across ESS is taken by considering the efficiencies for the power conversion during the charging and discharging processes. Since the ESS is charged through the DPP, the rate change of the stored energy in ESS is proportional to the net power supplied by the diesel power plant. Mathematically, it is the difference between power supplied by the DPP (X_{dg}) and the active power (X_i) consumed by the load at any time instant and is shown by equation (5).

Table 2 shows a typical load scenario of a house connected to the small community microgrid system. The uncontrollable loads include the common community loads like pump load, street light load, dispensary load, etc. A typical set of 24hr load demand data is considered for the study with half an hour data samples. The algorithms check and satisfy the load demand at each instant of the day, and hence,

the overall load curve obtained now has a controlled system peak.

$$(X_{dg} - X_i) * E = \frac{dQ_{ESS}}{dt} \quad (5)$$

$$where \begin{cases} E = \{\eta_c\} \text{ for } X_{dg} \geq X_i \\ E = \{1/\eta_d\} \text{ for } X_{dg} < X_i \end{cases} \quad (6)$$

E is the efficiency corresponding to charging and discharging processes. dQ_{ESS}/dt is the rate change of the stored energy in the ESS. η_c and η_d are charging and discharging efficiencies of the storage system, respectively. Stored energy (Q_{ESS}) in ESS over a time period Δt may be expressed by equation (7).

$$Q_{ESS}(t+\Delta t) = Q_{ESS}(t) + \int_t^{t+\Delta t} (X_{dg}(t) - X_i(t)) * E dt \quad (7)$$

For relatively small time periods the above equation can be approximated by equation (8):

$$Q_{ESS}(t + \Delta t) = Q_{ESS}(t) + (X_{dg}(t) - X_i(t)) * E \Delta t \quad (8)$$

Typical storage system parameters considered in this study are given in Table 3.

3. NUMERICAL CASE STUDY

A numerical case study has been performed for the two optimization conditions. In the first part (i.e., case 1), the optimization of the microgrid system is performed without the implementation of DSM. This means only the initial system peak is considered for the MG sizing. The second part (case 2) pertains to the MG sizing after the DSM execution when the system peak is reduced to a predefined dispatchable limit through the controllable loads. This also improves the power utilization of the connected loads as well as the overall load factor of the system. The equations (9)-(12) describe the available system constraints. The equations (9) and (12) show the load-demand constraint before and after the DSM execution, respectively. The other equations show the constraints on DERs maximum/minimum output. These constraints are utilized for our genetic algorithm implementation for optimization. Table 4 shows the typical maximum/minimum output ratings associated with each type of power plant under consideration.

3.1 The system constraints for case 1

- A fixed cost of electricity production is considered (location specific).
- A single unit of each type of DER plant.
-

$$X_{bat} + X_{dg} \geq X^{oldp} \quad \forall t \quad (9)$$

Table 2: Controllable and uncontrollable loads of a typical home

Device Name	Device Type	Rating (kW)	Operating hrs for Group1 loads	Operating hrs for Group2 loads	Operating hrs for Group3 loads	Operating hrs for Group4 loads	Operating hrs for Group5 loads
Washing Machine	controllable	1.4	1	1	1	1	1
A.C	controllable	1.2	0	0	0	0	0
Refrigerator	controllable	0.15	24	24	24	24	24
Lighting Loads	controllable	0.4	5	6	6	6	6
Fan	controllable	0.08	0	0	0	0	0
TV	controllable	0.09	5	4	6	6	6
Heating Loads	controllable	1.0	13	13	11	11	11
Remaining Loads	uncontrollable	3.2	24	24	24	24	24

Table 3: Typical Storage system Parameters

S.No	Parameters/quantity	Value/Number
1	η_c	0.9
2	η_d	0.9
3	ISOC	40 kW
4	ESS System	1(10kW for 4hrs)

Table 4: Plant max/min rating

Plant type	X^{max} (kW)	X^{min} (kW)
ESS	12	10
DPP	70	10

$$X_{bat}^{max} \geq X_{bat} \geq X_{bat}^{min} \quad \forall t \quad (10)$$

$$X_{bg}^{max} \geq X_{dg} \geq X_{dg}^{min} \quad \forall t \quad (11)$$

3.2 The system constraints for case 2

The constraints for case 2 are same as that of case 1, except the constraint given in the equation (9) changes to equation (12) with a new reduced system peak.

$$X_{bat} + X_{dg} \geq X^{newp} \quad \forall t; \quad (12)$$

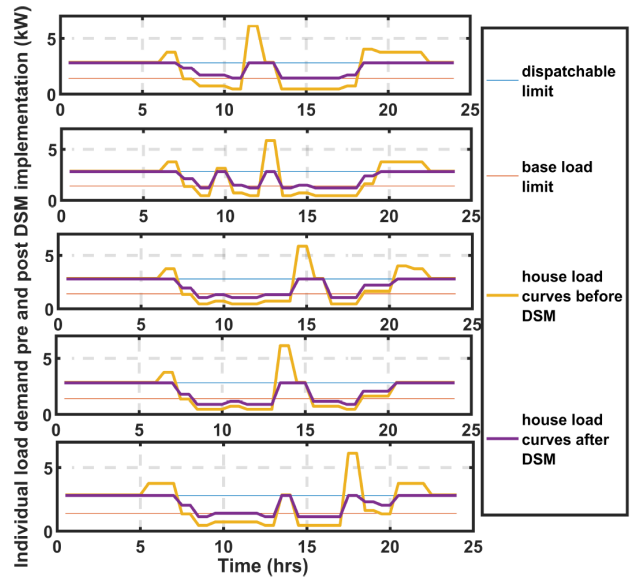
X^{oldp} and X^{newp} are the overall system peak before and after load alterations and are discussed in detail in the next section. X_{bat} , (kW) and X_{dg} (kW) are the output ratings of ESS and diesel generator system. X_{bat}^{max} , X_{bat}^{min} and X_{dg}^{max} , X_{dg}^{min} are the maximum and minimum output ratings of the ESS and diesel generator systems, respectively.

4. RESULTS & DISCUSSIONS

The overall energy management problem is formulated and analyzed with the help of the peak shaving strategy of DSM. This technique is applied on the individual load curve of the community houses in such a manner that each time the peak load crosses the

set dispatchable limit (shown in figure 7), the overall peak of the system shift towards regions where the load is comparatively low and this can be achieved through the smart appliances connected at the consumer's premises. Each curve in figure 7 shows the average value of multiple random load scenarios presented in figure 6. Figure 8 shows the overall system load curve, which is obtained before and after the implementation of demand response on the microgrid community load curve. It can be observed from the figure that the load curves settle to a predefined dispatchable limit after the execution of DSM through the applied algorithms.

The charging and discharging of the storage system, along with the implementation of DSM on the community load, can be seen from figure 9. It is observed from this figure that during the post DSM execution period, if the overall load curve reduces to a prescribed load limit, the energy from the DPP is used for ESS charging.

**Fig.7:** Individual load curve profile before and after DSM implementation

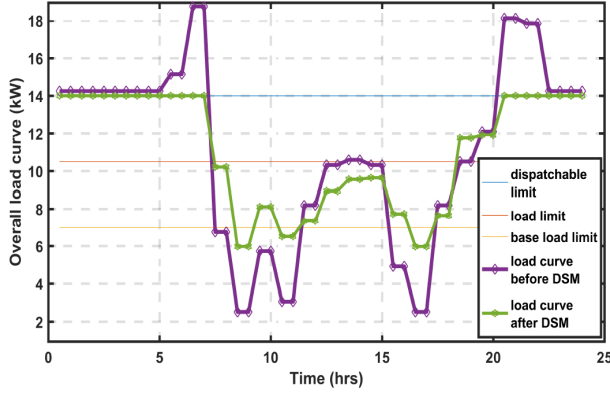


Fig.8: Overall load curve before and after DSM implementation

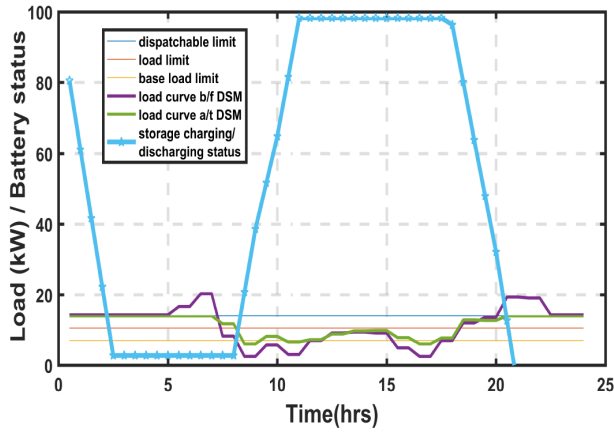


Fig.9: Overall load curve before and after DSM Implementation with ESS profile

It can be seen that during the morning hours, the controllable load is more than 15% of X_{dg} (load limit for battery charging/discharging) or the total load is greater than $0.85 X_{dg}$ and ESS is initially charged at its full capacity. Therefore, as per the algorithms, the discharging of the storage system up to a 30% of the DOD level starts. Thereafter, the battery system stays at this level until a charging region is created or the availability of energy for the charging is there, and then it charges through X_{dgr} (DPP reserve capacity) as per reliability considerations. After the seventh hour, the load starts decreasing, so the battery system gets charging through the diesel power plant until it acquires a maximum SOC set level of 90%. The charging area in the load curve is available up to 17:00 hrs. Later the load demand increases during the evening hours over a certain prescribed limit, and hence, the discharging process starts. The overall charging and the discharging of the ESS solely depends upon the applied algorithms.

The overall load of the microgrid system can be defined by the total available base-load. This base-load comes from the critical load of the system,

Table 5: Comparative optimal sizing and cost analysis of DERs

S.No	DER	X_a (kW) ^a		N_b ^b	
		Case1	Case2	Case1	Case2
1.	ESS	10	10	1	1
2.	DPP	56.74	52	6	5

^a Optimal Ratings

^b Optimal Number

which needs to be supplied continuously, and the non-critical load. Therefore, the base-load curve is added to the overall system peak before and after the implementation of DSM to obtain the overall microgrid load. Hence, the total load before the DSM execution can be obtained as $(18.75(\text{initial peak load in (kW)}) + 48 (\text{base-load in (kW)}))$ and is equal to 66.75kW (X_{oldp}) and the $(14 \text{ kW (peak after DSM)} + 48 \text{ kW (base-load)})$ which is equal to 62kW (X_{newp}) after the DSM implementation, respectively. Tables 5, 6, and 7 show the assessment of results with respect to various parameters for the cases 1 and 2. In Table 5, the optimal number of DERs to be connected in a typical plant is obtained for both DPP and ESS based power plants along with their optimal ratings. Table 6 shows a comparative assessment of results for GA as well as MILP based approaches for cases 1 and 2, respectively. It can be seen from the table that an annual cost savings of about \$ 3,318.00 can be achieved with our GA based approach. Also, the overall load factor of the system improved from 58.96% to 78.96%. It is also clear from the table that the MILP based approach provides an optimal cost reduction of \$ 3,485.00, which is higher than the GA based approach. Therefore, the other results are discussed for the GA only which provide comparatively more economical results compared to the MILP approach. Table 7 shows the CO_2 profile of the MG system for the aforementioned two cases. There is a reduction in the CO_2 emission observed of about $4.194e5 \text{ KgCO}_2/\text{year}$. The CO_2 emission calculations are made for fossil fuel-based DER. For example, DPP, with a consideration of 1.5 gallon/hr diesel consumption rate for the generator for both the cases. The CO_2 emission tax is considered as \$9/Ton.

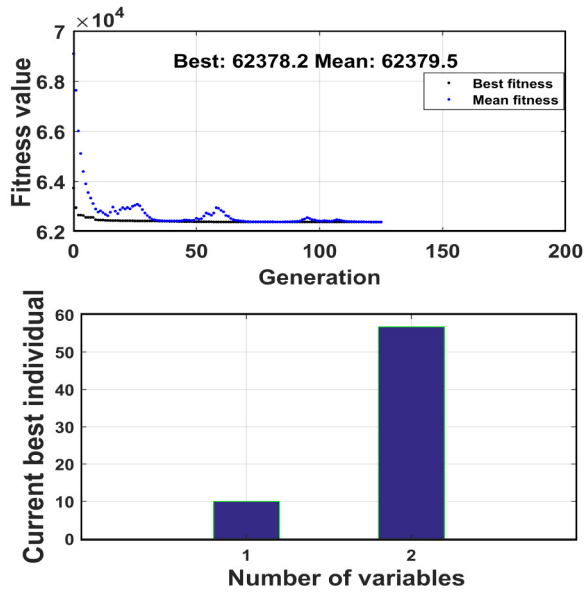
For case 1 before the DSM implementation, the overall system peak load was observed as 66.75kW . In this case, the optimal number of ESS units and diesel generator units in a given type of plant are observed as 1 and 6 with the optimal ratings of 10kW and 56kW , respectively. The optimal percentage use of the DPP is obtained as 81%, and the rest can be used as reserve capacity (X_{dgr}). The optimal cost in this case is \$ 6,237.80. The cost and the optimal values, in this case can be seen from figure 10. Similarly, for case 2 post DSM execution, the overall peak of the microgrid system is now reduced to a lower value. Therefore, the overall system sizing is

Table 6: A comparative cost and load factor assessment

S.No	Parameters	Case 1 (GA)	Case 2 (GA)	Case 1 (MILP)	Case 2 (MILP)
1.	Optimal cost (C_{opti})(\\$)	6,2378.00	5,9060.00	6,3241.00	5,9756.00
2.	Total reduction in optimal cost	3,318.00 (GA)		3,485.00 (MILP)	
3.	Load Factor (%)	58.96	78.964	58.96	78.964

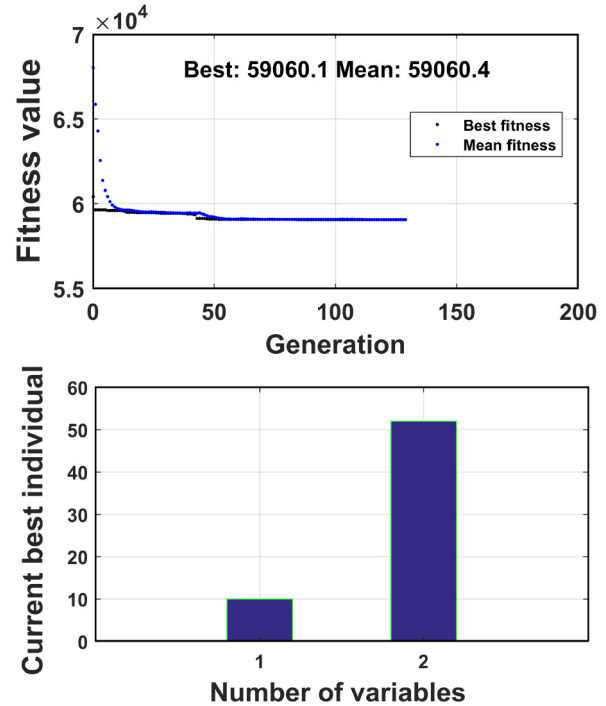
Table 7: CO_2 Profile

S.No	Parameters	Case 1 (GA)	Case 2 (GA)
1	CO_2 emission (Kg CO_2 /yr)	29.16e5	24.966e5
2	Total reduction in CO_2 emission	4.194e5	
3	Reduction in CO_2 tax (\\$/yr)	1,3420.00	

**Fig.10:** Best individual contribution of DERs for case1

done corresponding to 62kW, and not corresponding to 66.75kW. The optimal number of DERs required in a typical power plant for the aforementioned two cases changed to 1 and 5 from previous values of 1 and 6 with an individual optimal rating of 10kW and 52kW for the ESS and the DPP, respectively. The number of DERs in the DPP was reduced. Since the DPP is serving as a primary energy source and supplying a major part of the load and also the storage plant is only serving as a supporting energy source, this reduction is observed in DPP only and not in the storage plant. The microgrid optimal cost, in this case is, obtained as \\$ 5,9060.00, and can be seen in figure 11. The required optimal capacity of the DPP is also reduced to a value which is about 74% of the overall rated capacity of the plant and is 7% less than the first case. This also provides an additional scope for storage system charging and also saves the reserve capacity of the diesel power plant.

A reduction of 4.75kW in the peak load requirement has been observed after the implementation of DSM. The change in the optimal number of dis-

**Fig.11:** Best individual contribution of DERs for case2

tributed sources and its capacity depends upon the costs associated with them. The storage system plays a significant role in the working of the overall MG system. This not only ensures the reliable supply to the MG system but also encourages the use of many sustainable energy resources such as rooftop solar panels and small scale wind turbines. The average computational time for the algorithm to run for the considered microgrid system is observed as 4.9 sec. It is important to notice that the overall computational time largely depends upon the problem structure and the parameters included.

5. CONCLUSION

A cost-based planning scenario is considered that includes the net cost of all the DER based plants. The optimization problem is executed in a way that

starts from the forecasting of the community load to the implementation of the DSM technique on controllable load to the cost optimization for the two cases considered. The load uncertainty of 10-15% is added using a beta distribution. Since the community load is small, the two types of DERs are sufficient to supply the load. For bigger systems, locally available energy sources like solar and wind energy can also be utilized. The applied algorithms work in such a manner that each time the percentage contribution of an individual group load curve changes or violates the set dispatchable limit, the peak of the system will be shifted accordingly to the low load hours. The genetic algorithm is used to optimize the overall microgrid system. The results show the optimal sizing of DERs in a given MG system, including the optimal ratings of each DER as well as the optimal numbers of DERs required to connect in a particular power plant. In this study, a small scale MG test system is considered. The overall sizing of the system incorporates some critical aspects of forecasted data collection and its processing and the implementation of DSM on the system. The aforementioned algorithms are designed to work for a remote area community where main grid supply access is not available. These kinds of small scale community smart microgrids can be supplied using the formulated algorithms and can be beneficial. For the installation of supply systems for these small scale microgrids, comparatively smaller time horizons are required. The optimization problem is executed on a server with the Intel Core i7 vpro processor at 3.60 GHz processing speed with 24 GB of RAM. In the future, Plug-in hybrid electric vehicles (PHEV) can also be a part of such small scale smart microgrids.

References

- [1] K. Maneesh and T. Barjeev, "Long term microgrid planning based on lcc analysis for different system configurations," *IEEE Conf. IC-CPCCT*, pp. 52–56, 2018.
- [2] T. A. Hoverstad, Boye A, H. Langseth, and P. Ozturk, "Short-term load forecasting with seasonal decomposition using evolution for parameter tuning," *IEEE Transactions on Smart Grid*, vol. 6, no. 4, pp. 1904–1913, 2015.
- [3] M. Akole and B. Tyagi, "Artificial neural network based short term load forecasting for restructured power system," pp. 1–7, 2009.
- [4] H. Lotfi and A. Khodaei, "Ac versus dc microgrid planning," *IEEE Transactions on Smart Grid*, vol. 8, no. 1, pp. 296–304, 2017.
- [5] B. Jiang and Y. Fei, "Smart home in smart microgrid: A cost-effective energy ecosystem with intelligent hierarchical agents," *IEEE Transactions on Smart Grid*, vol. 6, no. 1, pp. 3–13, 2015.
- [6] M. Dale, "A comparative analysis of energy costs of photovoltaic, solar thermal, and wind electricity generation technologies," *Applied Sciences*, vol. 3, no. 2, pp. 325–337, 2013.
- [7] "Load generation balance report," *CEA, Annual Report*, pp. 1–127, 2016–17.
- [8] "International energy outlook 2017," *EIA*, pp. 1–76, 2017.
- [9] "India's intended nationally determined contributions-towards climate justice," *Ministry of Environment, Forest and Climate Change, Govt. of India*, pp. 1–28, 2015.
- [10] Y. L. Wenbo Qi, Jie Li. and C. Liu, "Planning of distributed internet data center microgrids," *IEEE Transactions on Smart Grid*, vol. 10, no. 1, pp. 762–771, 2019.
- [11] M. Husein and Y. Chung, "Evaluating investment in grid-connected microgrid under policy and technology risks," *International Conference on Electrical Machines and Systems (ICEMS)*, pp. 1–4, 2018.
- [12] H. Wang and J. Huang, "Cooperative planning of renewable generations for interconnected microgrids," *IEEE Transactions on Smart Grid*, vol. 7, no. 5, pp. 2486–2496, 2016.
- [13] B. D. Daniel Tenfen, Erlon C. Finardi and F. Wurtz, "Lithium-ion battery modelling for the energy management problem of microgrids," *IET Generation, Transmission Distribution*, vol. 10, no. 3, pp. 576–584, 2016.
- [14] D. R. Juan Clavier, Francois Bouffard and G. Joos, "Generation dispatch techniques for remote communities with flexible demand," *IEEE Transaction on Sustainable Energy*, vol. 6, no. 3, pp. 720–728, 2015.
- [15] W. Kong, Z. Y. Dong, D. J. Hill, F. Luo, and Y. Xu, "Short-term residential load forecasting based on resident behaviour learning," *IEEE Transactions on Power Systems*, vol. 33, no. 1, pp. 1087–1088, 2018.
- [16] A. Tajer, "Load forecasting via diversified state prediction in multi-area power networks," *IEEE Transactions on Smart Grid*, vol. 8, no. 6, pp. 2675–2684, 2017.
- [17] L. Li, K. Ota, and M. Dong, "When weather matters: Iot-based electrical load forecasting for smart grid," *IEEE Communications Magazine*, vol. 55, no. 10, pp. 46–51, 2017.
- [18] A. Ahmad, N. Javaid, M. Guizani, N. Alrajeh, and Z. A. Khan, "An accurate and fast converging short-term load forecasting model for industrial applications in a smart grid," *IEEE Transactions on Industrial Informatics*, vol. 13, no. 5, pp. 2587–2596, 2017.
- [19] Miao Sun and Xing He, "A recurrent neural network for optimal energy management considering the battery cycle-life in smart grid," *IEEE Int. Conf. on Information, Cybernetics, and Computational Social Systems (ICCSS)*, pp. 197–202, 2019.

- [20] B. Li, J. Zhang, Y. He, and Y. Wang, "Short-term load-forecasting method based on wavelet decomposition with second-order gray neural network model combined with adf test," *IEEE Access*, vol. 5, pp. 16324–16331, 2017.
- [21] F. K. Nima Amjady and H. Zareipour, "Short-term load forecast of microgrids by a new bilevel prediction strategy," *IEEE Transaction on Sustainable Energy*, vol. 1, no. 3, pp. 286–294, 2010.
- [22] L. Hernandez and C. Baladron, "A survey on electric power demand forecasting: Future trends in smart grids, microgrids and smart buildings," *IEEE Communications Surveys Tutorials*, vol. 16, no. 3, pp. 1460–1495, 2014.
- [23] J. K. G. Barry P. Hayes and M. Prodanovic, "Multi-nodal short-term energy forecasting using smart meter data," *IET Generation, Transmission Distribution*, vol. 12, no. 12, pp. 2988–2994, 2018.
- [24] M. H. Albadi and E. F. El-Saadany, "Demand response in electricity markets: An overview," *IEEE Power Engineering Society General Meeting*, pp. 1–5, 2007.
- [25] H. Wang and J. Huang, "Joint investment and operation of microgrid," *IEEE Transactions on Smart Grid*, vol. 8, no. 2, pp. 833–845, 2017.
- [26] R. Rigo-Mariani, B. Sareni, and X. Roboam, "Integrated optimal design of a smart microgrid with storage," *IEEE Transactions on Smart Grid*, vol. 8, no. 4, pp. 1762–1770, 2017.
- [27] Lokeshgupta Bhamidi and S. Sivasubramani, "Optimal Planning and Operational Strategy of a Residential Microgrid With Demand Side Management," *IEEE Systems Journal*, vol. 14, no. 2, pp. 2624–2632, 2020.
- [28] Guolong MA, Z. Cai et, al, "A Bi-Level Capacity Optimization of an Isolated Microgrid With Load Demand Management Considering Load and Renewable Generation Uncertainties," *IEEE Access*, pp. 1–14, 2019.
- [29] S. Haghifam, K. Zare, and M. Dadashi, "Bi-level operational planning of microgrids with considering demand response technology and contingency analysis," *IET Gen. Trans. & Dist.*, vol. 13, no. 13, pp. 2721–2730, 2019.
- [30] J. Mitra, M. R. Vallem, and C. Singh, "Optimal deployment of distributed generation using a reliability criterion," *IEEE Transactions on Industry Applications*, vol. 52, no. 3, pp. 1989–1997, 2016.
- [31] K. Maneesh and T. Barjeev, "A state of art review of microgrid control and integration aspects," *IEEE conf. IICPE*, 2016.
- [32] L. Guo, W. Liu, B. Jiao, B. Hong, and C. Wang, "Multi-objective stochastic optimal planning method for stand-alone microgrid system," *IET Gen. Trans. & Dist.*, vol. 8, no. 7, pp. 1263–1273, 2014.
- [33] Omer Faruk Ertuerul and Ramazan Tekinand, "Randomized feed-forward artificial neural networks in estimating short-term power load of a small house:a case study," *IEEE Int. Conf.*, pp. 1–5, 2017.
- [34] R. Banerjee, "Comparison of options for distributed generation in india," *Energy Policy*, vol. 34, no. 1, pp. 101–111, 2006.
- [35] A. Nayak, "Cost economics of solar kwh,' national productive council," *National productive council, Report*, pp. 1–4, 2012.
- [36] "Renewable power generation costs report," *IRENA*, pp. 1–158, 2017.
- [37] K. Maneesh and T. Barjeev, "Capital cost based planning and optimal sizing of a small community smart microgrid," *IEEE Conf. KST*, pp. 121–126, 2020.
- [38] K. Maneesh and T. Barjeev, "An optimal multi-variable constrained nonlinear (mvcnl) stochastic microgrid planning and operation problem with renewable penetration," *IEEE Systems Journal*, vol. 14, no. 3, pp. 4143–4154, 2020.



Maneesh Kumar received his B-Tech degree in electrical engineering from G.B Pant University, Pantnagar, India, and his master's degree in electrical engineering from PEC University of Technology, Chandigarh, India, in 2009 and 2015, respectively. He is currently completing his Ph.D. degrees in power system engineering from the Indian Institute of Technology Roorkee, India. He is a member of many professional societies, viz. IEEE, ISTE, IEI, and SESI, etc. His area of research includes microgrids, smart grids, renewable energy systems, distributed generation, optimization, etc.



Barjeev Tyagi received his B.E. degree in electrical engineering from the Indian Institute of Technology, Roorkee, India (formerly University of Roorkee), in 1987, the M.Tech. degree in electrical engineering (control system) from the Indian Institute of Technology, Kharagpur, India, in 2000, and the Ph.D. degree in electrical engineering from the Indian Institute of Technology, Kanpur, India, in 2005. Since 2007, he is serving as a Professor with the Department of Electrical Engineering, Indian Institute of Technology, Roorkee. His research interests include wide-area power system monitoring and control, distributed generation, power system deregulation, microgrid operation, and control.